Autoresonance laser accelerator

A. Loeb
Center for Plasma Physics, Racah Institute of Physics, Hebrew University of Jerusalem, 91904 Jerusalem, Israel and Plasma Department, Soreq Nuclear Research Center, 70600 Yavne, Israel

L. Friedland
Center for Plasma Physics, Racah Institute of Physics, Hebrew University of Jerusalem, 91904 Jerusalem, Israel
(Received 7 August 1985)

A laser-electron-acceleration scheme based on self-sustained cyclotron resonance is discussed. Nonlinear electron dynamics in combined axisymmetric magnetic and transverse laser radiation fields is investigated. Analytic solutions are given for a circularly polarized luminous ($\omega/ck=1$) radiation case, which allows time unlimited phase locking between the electrons and the accelerating electromagnetic wave. An appropriate tapering of the magnetic field in the superluminous case ($\omega/ck>1$) can also lead to significant accelerations, restricted by the maximum available strength of the guide magnetic field. We discuss the entrance conditions for the accelerated beam as well as its launching into the desirable autoresonance regime through a transition region. It is shown that the radiation losses in a 1-TeV accelerator are negligible. Also, high-current-beam acceleration seems to be feasible. Nd-glass lasers with intensity of 10^{18} W/cm^2 are capable of accelerating high-current electron beams from 0.25 to 2.5 GeV over 1 m by using a 100-kG guide magnetic field.

I. INTRODUCTION

Recently, there has been much interest in increasing the present maximum acceleration gradients of several tens of MeV/m, by using high-power lasers.[1] Due to the limitations on coherent radiation power levels which can be guided without inducing breakdown on the waveguide walls, several new laser acceleration schemes were proposed in the last years. For example, plasma-beat-wave accelerators[2-5] (PBWA) are based on excitation of large-amplitude plasma electrostatic waves by intense electromagnetic radiation. The plasma wave is used for accelerating charged particles moving in phase with it. Although theoretically feasible, the beat-wave approach suffers from competing plasma instabilities[4] and technological difficulties, such as constrains on the uniformity of the plasma and fine tuning between the beat-wave frequency of the laser and the plasma frequency.[5] On the other hand, such schemes as the inverse free-electron-laser accelerator[6] (IFEL) have limitations due to radiation losses and complex tapered wiggler configurations. In addition, phasing problems and interactions between the plasma wave and the electron beam in PBWA and transverse gradients of the wiggler field in IFEL impose a restriction on the maximum electron-beam current.

In this paper we consider an acceleration scheme based on cyclotron autoresonance. The concept, in principle, allows acceleration of charged particles moving in phase with a rotating electromagnetic field along an axisymmetric magnetic field,[7] namely satisfying the condition $k_0 v_z-\omega_0'-\Omega'/\gamma=0$, where k_0 and ω_0' are the laser wave vector and frequency and γ and v_z are the relativistic factor and axial velocity of the particles. Recently, an autoresonance accelerator based on a nonpropagating ($k_0=0$) electromagnetic wave was discussed.[8] This accelerator cannot be extended to ultrahigh energies because of radiation losses of the accelerated particles. Here, we reconsider an autoresonance acceleration scheme with a traveling electromagnetic wave for the following reasons. One usually expects the charged particles to satisfy the resonance condition and stay in phase with the rotating accelerating field by moving in an approximate helical trajectory with a slowly varying γ. However, our recent study of the nonlinear dynamics of electrons in the mentioned configuration of fields showed that, in general, the electrons follow nonhelical trajectories. Only for very specific entrance conditions can one achieve a helical equilibrium. Moreover, for the same set of parameters (ω_0', k_0, Ω', γ, and laser intensity) there exist several different helical equilibria, some of which are unstable. This complexity is similar to that found in free-electron-laser applications[9] (in fact, the latter situation is a special case of a wave with $\omega_0'=0$). In view of these new results, the present study will consider the autoresonance laser accelerator (ALA) emphasizing issues such as the nonlinear particle dynamics, the ways of launching the beam into the proper autoresonance condition, and the acceleration of large radii high-current-electron beams, arising due to the uniformity of the guide magnetic field.

The presentation will be as follows. In Sec. II the nonlinear electron-beam dynamics in combined axisymmetric guide magnetic field and laser radiation is investigated. An analytical solution is given for circularly polarized luminous radiation ($\omega_0'/ck_0=1$), and constant magnitudes of the fields. It is shown that the resonance condition is preserved along the electron trajectory if it is satisfied initially. In the same section we will show that an appropriate tapering of the axisymmetric magnetic field yields acceleration for the superluminous case [$(\omega_0'/ck_0)>1$]. In Sec. III the entrance conditions for the

electron beam and its launching through a transition region are discussed. Radiation losses and collective effects at high currents are considered in Sec. IV. Finally, conclusions are summarized in Sec. V.

II. ELECTRON-BEAM DYNAMICS IN COMBINED AXISYMMETRIC GUIDE MAGNETIC FIELD AND TRANSVERSE ELECTROMAGNETIC RADIATION

Consider a plane electromagnetic wave propagating in the z direction along an axisymmetric weakly inhomogeneous magnetostatic field $\mathbf{B}_0(z,r)$. Let $\mathbf{k}_0$, ω_0' be the wave vector and the frequency of the wave, respectively. Define the following orthonormal set of vectors:

$$\begin{aligned}\hat{\mathbf{e}}_1&=-\hat{\mathbf{e}}_x\sin\phi+\hat{\mathbf{e}}_y\cos\phi\ ,\\ \hat{\mathbf{e}}_2&=-\hat{\mathbf{e}}_x\cos\phi-\hat{\mathbf{e}}_y\sin\phi\ ,\\ \hat{\mathbf{e}}_3&=\hat{\mathbf{e}}_z\ ,\end{aligned}\tag{1}$$

where

$$\phi=k_0z-\omega_0't\ .$$

Assuming circular polarization, one can write the electromagnetic fields in the system as

$$\begin{aligned}\mathbf{E}&=-\frac{1}{c}\frac{\partial\mathbf{A}}{\partial t}\ ,\\ \mathbf{B}&=\nabla\times\mathbf{A}+B_z\hat{\mathbf{e}}_3-\frac{1}{2}\frac{\partial B_z}{\partial z}\mathbf{r}=\nabla\times\mathbf{A}+\mathbf{B}_0\ ,\end{aligned}\tag{2}$$

where $\mathbf{r}=r_1\hat{\mathbf{e}}_1+r_2\hat{\mathbf{e}}_2$ is the radius vector and

$$\mathbf{A}=A_0\hat{\mathbf{e}}_2\ .\tag{3}$$

We shall discuss here the dynamics of a cold relativistic electron beam in the above-mentioned field configuration, assuming that $\mathbf{E}$ and $\mathbf{B}$ are large enough to be affected by the beam itself. The electron momentum equation is

$$\left[\frac{\partial}{\partial t}+\mathbf{v}\cdot\nabla\right](m\gamma\mathbf{v})=-e\left[\mathbf{E}+\frac{\mathbf{v}}{c}\times\mathbf{B}\right]\ ,\tag{4}$$

where $\gamma=(1-v^2/c^2)^{-1/2}$. Equivalently by using Eq. (2)

$$\left[\frac{\partial}{\partial\tau}+\mathbf{u}\cdot\nabla\right](\gamma\mathbf{u}-\boldsymbol{\alpha})=\left[\boldsymbol{\Omega}-\frac{1}{2}\frac{d\Omega}{dz}\mathbf{r}\right]\times\mathbf{u}-(\nabla\boldsymbol{\alpha})\cdot\mathbf{u}\ ,\tag{5}$$

where we use the following notation:

$$\omega_0\equiv\omega_0'/c,\quad \tau\equiv ct,\quad \mathbf{u}=\mathbf{v}/c,\quad \boldsymbol{\Omega}=(eB_z/mc^2)\hat{\mathbf{e}}_z$$

and

$$\boldsymbol{\alpha}=e\mathbf{A}/mc^2=\alpha_2\hat{\mathbf{e}}_2,\quad \alpha_2=eE/m\omega_0'c\ .$$

Next, we write Eq. (5) in components,

$$\frac{d}{d\tau}(\gamma u_1)=-\Omega u_2-(\omega_0-u_3k_0)(\gamma u_2-\alpha_2)-\left[\frac{1}{2}\frac{\partial\Omega}{\partial z}\right]r_2u_3\ ,\tag{6}$$

$$\frac{d}{d\tau}(\gamma u_2)=\Omega u_1+(\omega_0-u_3k_0)(\gamma u_1)+u_3\frac{\partial\alpha_2}{\partial z}+\left[\frac{1}{2}\frac{\partial\Omega}{\partial z}\right]r_1u_3\ ,\tag{7}$$

$$\frac{d}{d\tau}(\gamma u_3)=k_0\alpha_2u_1-u_2\frac{\partial\alpha_2}{\partial z}+\left[\frac{1}{2}\frac{\partial\Omega}{\partial z}\right](r_2u_1-r_1u_2)\ ,\tag{8}$$

where it is assumed that $\partial\alpha_2/\partial\tau=0$. The electron transverse position obeys

$$\begin{aligned}\frac{dr_1}{d\tau}&=u_1-(\omega_0-u_3k_0)r_2\ ,\\ \frac{dr_2}{d\tau}&=u_2+(\omega_0-u_3k_0)r_1\ ,\end{aligned}\tag{9}$$

and its axial position is determined via

$$z=\int u_3d\tau\ .\tag{10}$$

Finally, the energy of the electron beam is given by

$$\frac{d\gamma}{d\tau}=\omega_0\alpha_2u_1\ .\tag{11}$$

Equations (6)—(11) describe the dynamics of the electrons in the above-mentioned fields configuration.

First, we will consider a homogeneous situation $[(d\Omega/dz)=(d\alpha_2/dz)=0]$ described by

$$(\gamma u_1)^{\cdot}=au_2+k_0\alpha_2(u_p-u_3)\ ,\tag{12}$$

$$(\gamma u_2)^{\cdot}=-au_1\ ,\tag{13}$$

$$(\gamma u_3)^{\cdot}=k_0\alpha_2u_1=\frac{\dot{\gamma}}{u_p}\ ,\tag{14}$$

where $(\ )^{\cdot}\equiv d/d\tau$, $u_p\equiv\omega_0/k_0$, $\gamma=(1-u_1^2-u_2^2-u_3^2)^{-1/2}$, and

$$a\equiv k_0\gamma(u_3-u_p)-\Omega\ .\tag{15}$$

Equations (12) and (13) yield a steady-state helical equilibrium with: $u_1\equiv0$, $u_3,\gamma=$const, and

$$u_2=\frac{k_0\alpha_2(u_3-u_p)}{a}=\text{const}\ .\tag{16}$$

The axial velocity is then found from

$$1-u_3^2-\left[\frac{k_0\alpha_2(u_3-u_p)}{a}\right]^2=\frac{1}{\gamma^2}\ ,\tag{17}$$

which is a fourth-order polynomial equation for u_3, for given α_2, k_0, u_p, Ω, and γ. Helical trajectories defined by (17) have been studied recently[10] in relation to an electromagnetically pumped free-electron laser with guide magnetic field. As was mentioned in the Introduction, these helical orbits are rather an exception than a rule and only special initial conditions on the electron beam lead it into one of these steady states. Nevertheless it can be easily understood that the described helical equilibria cannot be used in an autoresonance acceleration scheme. Indeed,

since $u_1 \equiv 0$ in the helical steady state, $\dot{\gamma} \equiv 0$. Also, Fig. 1 shows solutions of Eq. (17) for u_3 as a function of Ω for $\alpha_2 = 0.3$, $k_0 = 15$ cm^{-1}, $\gamma = 3$, and $u_p = 1.05$. The dot-dashed line in this figure represents the resonance condition $a = 0$ and indicates that resonance is never achieved in the steady state. Thus, we conclude that the steady states can only be used in a different scheme than the ALA scheme. One of the possibilities is the IFEL configuration where an additional perturbing electromagnetic wave is employed to accelerate electrons initially launched into an appropriate steady state. Consideration of this scheme, however, is out of the scope of the present work. Instead, we will consider another class of solutions of Eqs. (12)–(14).

Note first, that Eq. (14) yields the following constant of motion:

$$L_0 \equiv \gamma(1 - u_p u_3) = \text{const} . \tag{18}$$

Equation (18) predicts a possibility of $\gamma \to \infty$ if the solution

$$u_3 \to u_p^{-1} \tag{19}$$

is allowed by the momentum equation. The latter is only possible for luminous ($u_p = 1$) or superluminous ($u_p > 1$) waves.

Consider first the luminous case. Here Eqs. (12)–(14) become

$$(\gamma u_1)^{\cdot} = a_0 u_2 + k_0 \alpha_2 (1 - u_3) , \tag{20}$$

$$(\gamma u_2)^{\cdot} = -\frac{a_0}{k_0 \alpha_2} \dot{\gamma} , \tag{21}$$

$$(\gamma u_3)^{\cdot} = \dot{\gamma} = k_0 \alpha_2 u_1 , \tag{22}$$

where

$$a_0 \equiv -k_0 L_0 - \Omega = \text{const} . \tag{23}$$

Equation (21) now yields an additional constant of motion,

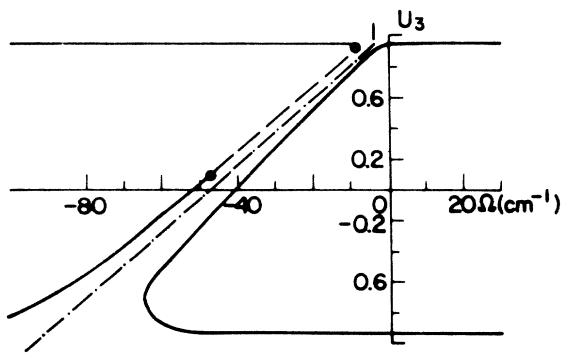

FIG. 1. Axial velocity u_3 vs Ω for a helical steady state with $\alpha_2 = 0.3$, $\gamma = 3$, $k_0 = 15$ cm^{-1}, and $u_p = 1.05$. The dashed line indicates unstable solutions. The dot-dashed line represents the cyclotron resonance, namely $u_3 = u_p + \Omega/(k_0 \gamma)$.

$$L_1 \equiv \gamma \left[u_2 + \frac{a_0}{k_0 \alpha_2} \right] = \text{const} , \tag{24}$$

so that

$$\lim_{\gamma \to \infty} u_2 = -\frac{a_0}{k_0 \alpha_2} . \tag{25}$$

Thus, according to (19) and (25), γ can be increased indefinitely in the luminous case only if $a_0 \equiv 0$. This is precisely the autoresonance condition, suitable for the acceleration purposes. Indeed, since a_0 is a constant of motion, it will remain zero for $\tau > 0$, if the electron is characterized by $a_0 = 0$ at $\tau = 0$. We do not have to change the parameters of the accelerator in this regime (as is done, for example, in the IFEL scheme) in order to reach the limit $\gamma \to \infty$. Although the ideal autoresonance situation is most important we will consider the general case of $a_0 \neq 0$ in the following discussion. This general solution will later allow evaluating the influence of perturbations (such as the effect of thermal spread in the energy of the electrons) on the performance of the ALA.

Combined Eqs. (20), (22), and (24) yield the following differential equation for the time evolution of γ:

$$2a_0^2 \gamma + (\gamma^2)^{\cdot\cdot} \gamma = 2k_0 \alpha_2 (a_0 L_1 + k_0 \alpha_2 L_0) \tag{26}$$

subject to the following initial conditions: $\gamma(\tau = 0) = \gamma_0$, $\dot{\gamma}(\tau = 0) = k_0 \alpha_2 u_{10}$. This equation has a solution,

$$\tau = \frac{(B_3 \gamma^2 + B_2 \gamma + B_4)^{1/2}}{B_3} + \frac{B_2}{2B_3(-B_3)^{1/2}} \arcsin \left[\frac{2B_3 \gamma + B_2}{(B_2^2 - 4B_3 B_4)^{1/2}} \right] - B_5 , \tag{27}$$

where

$$\begin{aligned} B_2 &= 8k_0 \alpha_2 (a_0 L_1 + k_0 \alpha_2 L_0) , \\ B_3 &= -4a_0^2 , \\ B_4 &= B_3 \gamma_0^2 + B_2 \gamma_0 - (2\gamma_0 k_0 \alpha_2 u_{10})^2 , \\ B_5 &= \frac{(B_3 \gamma_0^2 + B_2 \gamma_0 + B_4)^{1/2}}{B_3} + \left[\frac{B_2}{4a_0 B_3} \right] \arcsin \left[\frac{2B_3 \gamma_0 + B_2}{(B_2^2 - 4B_3 B_4)^{1/2}} \right] . \end{aligned} \tag{28}$$

Note that the acceleration rate is found by integration of Eq. (26),

$$\dot{\gamma} = \frac{1}{2\gamma} (B_3 \gamma^2 + B_2 \gamma + B_4)^{1/2} . \tag{29}$$

Thus, for $a_0 \neq 0$ ($B_3 \neq 0$), γ has a maximum value of

$$\gamma_m = \frac{B_2 + (B_2^2 + 16a_0^2 B_4)^{1/2}}{8a_0^2} , \tag{30}$$

and therefore,

$$\lim_{a_0 \to 0} \gamma_m a_0^2 = 2k_0 \alpha_2 (a_0 L_1 - \alpha_2 \Omega) = \text{const} . \tag{31}$$

For example, for $a_0 \ll 50\ \mathrm{cm}^{-1}$, $u_{10}=u_{20}=0$, and laser wavelengths in the range 1 μm–1 mm, one gets

$$mc^2\gamma_m\ (\mathrm{TeV})=4\frac{\alpha_2^2}{\lambda_0\ (\mu\mathrm{m})}\frac{B_z\ (100\ \mathrm{kG})}{[a_0\ (\mathrm{cm}^{-1})]^2}\ . \tag{32}$$

Therefore, for $B_z=100$ kG and $\alpha_2=1$ one should keep $|a_0|<0.06\ \mathrm{cm}^{-1}$ for millimeter waves ($\lambda_0=1$ mm) and $|a_0|<2\ \mathrm{cm}^{-1}$ for a Nd-glass laser ($\lambda_0=1\ \mu$m) in order to reach the TeV energies.

Let us consider now the autoresonance regime[7] ($a_0=0$), in which Eq. (26) yields

$$\tau=(A_1\gamma+A_2)^{1/2}(A_3\gamma-A_4)-A_5\ , \tag{33}$$

where

$$\begin{aligned} A_1&=8k_0^2\alpha_2^2L_0\ ,\\ A_2&=(2\gamma_0k_0u_{10}\alpha_2)^2-A_1\gamma_0\ ,\\ A_3&=4/3A_1\ ,\\ A_4&=8A_2/3A_1^2\ ,\\ A_5&=(A_1\gamma_0+A_2)^{1/2}(A_3\gamma_0-A_4)\ . \end{aligned} \tag{34}$$

It also follows from (29) that

$$\dot{\gamma}=\frac{1}{2}\left[\frac{A_1}{\gamma}+\frac{A_2}{\gamma^2}\right]^{1/2} \tag{35}$$

and γ can be increased indefinitely. The last equation yields the following solution for the velocity components:

$$u_1=\frac{1}{2k_0\alpha_2}\left[\frac{A_1}{\gamma}+\frac{A_2}{\gamma^2}\right]^{1/2}\ , \tag{36}$$

$$u_2=\frac{\gamma_0u_{20}}{\gamma}=\frac{L_1}{\gamma}\ , \tag{37}$$

$$u_3=1-\frac{L_0}{\gamma}\ . \tag{38}$$

Asymptotically, for $\gamma\gg\gamma_0$ we have

$$\gamma\cong(\tau/\tau_0)^{2/3}\ , \tag{39}$$

$$u_1\cong(2L_0/\gamma)^{1/2}\ , \tag{40}$$

where

$$\tau_0^{-1}=\frac{3}{\sqrt{2}}k_0\alpha_2(L_0)^{1/2}=3\alpha_2\left[\frac{|\Omega|k_0}{2}\right]^{1/2}\ , \tag{41}$$

and the maximum value of τ_0^{-1} is dictated by the maximum available strengths of the axial guide and laser radiation fields. For example, Fig. 2 shows γ versus z in the luminous case, found on using Eqs. (10) and (33), for different wavelengths $B_z=100$ kG and $\alpha_2=1$. As can be seen in these examples, acceleration gradients of several GeV/m in the first 100 cm of acceleration are feasible.

Next, we will consider the superluminous case. For $u_p>1$ (e.g., a wave propagating in a plasma or a wave guide) the axisymmetric magnetic field can be tapered so that one satisfies the resonance condition

$$\Omega\equiv k_0\gamma(u_3-u_p)\ . \tag{42}$$

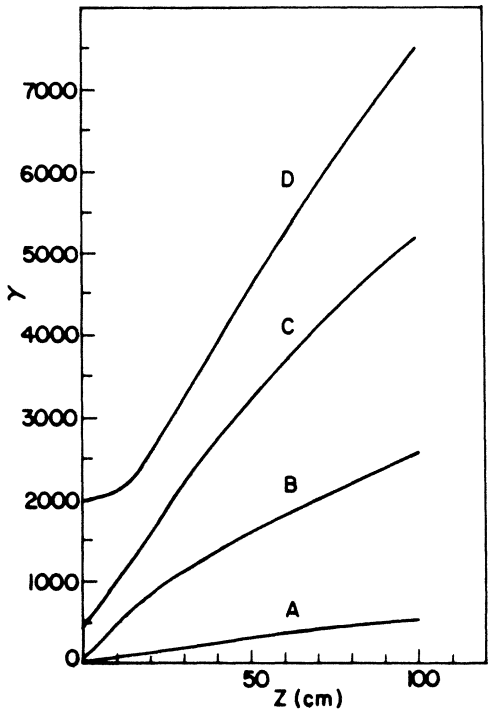

FIG. 2. Autoresonance acceleration in homogeneous fields for the luminous case ($u_p=1$) with $B_z=100$ kG, $\alpha_2=1$, $u_{10}=u_{20}=0$, and different laser wavelengths (λ_0). *A*, $\gamma_0\simeq1$, $\lambda_0=1$ mm; *B*, $\gamma_0=50$, $\lambda_0=10\ \mu$m (CO_2 laser); *C*, $\gamma_0=500$, $\lambda_0=1\ \mu$m (Nd-glass laser); *D*, $\gamma_0=2000$, $\lambda_0=0.25\ \mu$m (KrF laser).

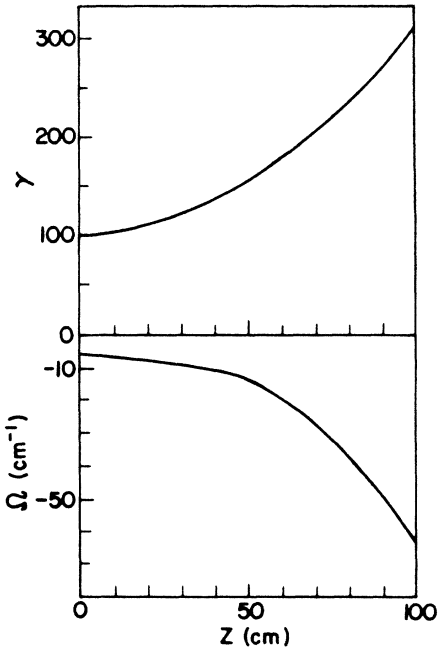

FIG. 3. Acceleration in the superluminous case ($u_p>1$) for $\lambda_0=1$ mm, $\alpha_2=1$, $u_{10}=u_{20}=0$, $\gamma_0=100$, $r_{10}=r_{20}=0.1$ cm, and $u_p=1.001$. The lower part of the figure shows tapering of the magnetic field necessary for satisfying the resonance condition.

Thus, it should be required that

$$\dot{\Omega}=u_3\frac{d\Omega}{dz}=k_0(\gamma u_3)^{\cdot}-\omega_0\dot{\gamma}$$

and Eqs. (8) and (11) yield

$$\frac{d\Omega}{dz}=\frac{k_0^2(1-u_p^2)\alpha_2 u_1-k_0u_2(d\alpha_2/dz)}{u_3+k_0(r_1u_2-r_2u_1)/2}\ . \tag{43}$$

In this case γ is limited by the maximum available strength of the axial magnetic field. Figure 3 shows the appropriate tapering of the guide field according to Eqs. (6)–(10), (43) for $\gamma_0=100$, $\lambda_0=1$ mm, $\alpha_2=1$, and $u_p-1=10^{-3}$. Also in the same figure the corresponding dependence of γ on z is given.

III. ENTRANCE CONDITIONS AND TRANSITION REGIONS

In this section we discuss the initial parameters of the electron beam, suitable for the ALA scheme, and the ways of launching the beam into the proper autoresonance regime.

According to Eqs. (39)–(41), initial beam parameters do not effect the advanced ($\gamma\gg\gamma_0$) autoresonance acceleration regime for fixed values of Ω_0, k_0, and α_2. Nevertheless, the acceleration rate increases as Ω_0, k_0, or α_2 increases. Since, in general, $0<L_0<1$, the initial value of γ necessary for satisfying the resonance condition, decreases as Ω_0 approaches k_0. In particular, for $\Omega_0=k_0$ this value should be 1. Note that the accelerated beam does not necessarily have an initial perpendicular velocity. If $u_{10}=0$, then according to Eq. (36),

$$\dot{u}_1=\frac{|\Omega_0|\alpha_2}{\gamma^2}\left[\frac{2\gamma_0}{\gamma}-1\right]\ . \tag{44}$$

Therefore u_1 grows until $\gamma=2\gamma_0$ to a maximum value of

$$(u_1)_{\max}=(2)^{-1/2}(1-u_{30})^{1/2}\ , \tag{45}$$

yielding a maximum acceleration rate of

$$(\dot{\gamma})_{\max}=k_0\alpha_2\left[\frac{1-u_{30}}{2}\right]^{1/2}\ , \tag{46}$$

so that for $\gamma_0\gg1$, one gets $(\dot{\gamma})_{\max}\cong k_0\alpha_2/2\gamma_0$.

Next we consider the transition regions. Assume that the particles enter and leave the homogeneous fields region (see Sec. III) by passing a transition region with slowly varying amplitude of the radiation field. In these regions, Ω should be varied so as to satisfy the resonance condition $a=0$. The appropriate tapering of the guide field is found from (43). For luminous radiation ($u_p=1$),

$$\frac{d\Omega}{dz}=-\left[\frac{k_0u_2}{[u_3+\frac{1}{2}k_0(r_1u_2-r_2u_1)]}\right]\left[\frac{d\alpha_2}{dz}\right]\ . \tag{47}$$

Since $u_{20}=0$ and $u_2\ll u_3$ in this case, one gets from Eq. (7):

$$(\gamma u_2)^{\cdot}\cong u_3\frac{d\alpha_2}{dz}=\dot{\alpha}_2\ , \tag{48}$$

and therefore $u_2\cong(\alpha_2/\gamma)$ in Eq. (47). For Ω varying according to Eq. (47) and taking $a_0=0$ initially, the electrons are accelerated along the transition region and arrive into the homogeneous region in the appropriate autoresonance condition. For example, Fig. 4 shows the variation in γ and B_z for an amplitude variation of the electromagnetic radiation of the form $\alpha_2=\alpha_0\exp\{-[(z-z_0)/\lambda]^2\}$ where $\alpha_0=1$, $z_0=100$ cm, and $\lambda=25$ cm. One can see (for $z<z_0$) that the autoresonance acceleration regime is readily achieved and (for $z>z_0$) one also succeeds to conveniently extract the accelerated beam from the interaction region.

Finally, we consider the effect of a spread in the initial conditions in the beam. Let the electron energy distribution function be centered around γ_0 with a spread range of $\Delta\gamma_0$. Assume also that the cyclotron frequency characterizing the guide field is Ω_0 with a maximum perturbation range of $\Delta\Omega_0$. Let the resonance condition $a_0=0$ be satisfied for γ_0 and Ω_0. Then, for $u_p=1$, $\gamma_0\gg1$ one gets [see Eq. (23)]

$$\frac{\Delta a_0}{k_0}=\frac{\Delta\gamma_0}{2\gamma_0^2}-\frac{\Delta\Omega_0}{k_0}\ . \tag{49}$$

At this point we can employ the analytic solutions for $a_0\neq0$ derived in Sec. II. In particular, we use Eq. (31) to calculate the allowed $\Delta\gamma_0$, $\Delta\Omega_0$ for given acceleration requirements. For example, according to Eq. (32), a 1 TeV autoresonance laser accelerator can be designed with a Nd-glass laser ($\lambda_0=1$ μm), $\gamma_0=500$, $B_z=100$ kG provided that $\Delta\gamma_0<10$ and $|\Delta B_z|<1$ kG. These restrictions on the beam quality and the homogeneity of the magnetic field are quite reasonable. Perturbations in α_2 do not cause a significant change in a_0 because they appear in the term $u_2(d\alpha_2/dz)$ in Eq. (8), which is small since $u_2\ll1$.

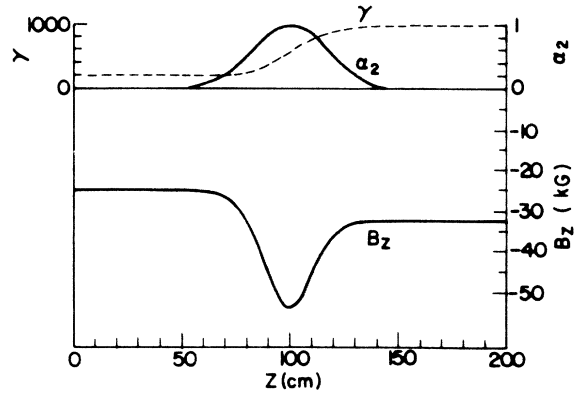

FIG. 4. Electron beam launching and extraction by using a tapered electromagnetic wave. The tapering of the magnetic field is necessary for satisfying the resonance condition at all stages. For all the curves: $\gamma_0=200$, $\lambda_0=10$ μm, and $\alpha_2=1$.

IV. RADIATION LOSSES AND SPACE-CHARGE EFFECTS AT HIGH CURRENTS

In this section we evaluate radiation losses and radial space charge effects on the acceleration process. The total power, in units of mc^2, emitted by a single electron is given by[11]

$$P_0=\frac{2r_e}{3}\gamma^6\left[\left|\frac{d\mathbf{u}}{d\tau}\right|^2-\left|\mathbf{u}\times\frac{d\mathbf{u}}{d\tau}\right|^2\right], \tag{50}$$

where $r_e=e^2/mc^2$ is the classical radius of the electron. Therefore, the ratio between the radiation losses and the energy-gain rate of the electron is

$$\delta=\frac{p_0}{\dot{\gamma}}=\frac{p_0}{\omega_0\alpha_2 u_1}. \tag{51}$$

Using the relation

$$\frac{d\mathbf{u}}{d\tau}=[\dot{u}_1-k_0(u_3-u_p)u_2]\hat{\mathbf{e}}_1 +[\dot{u}_2+k_0(u_3-u_p)u_1]\hat{\mathbf{e}}_2+\dot{u}_3\hat{\mathbf{e}}_3, \tag{52}$$

one can calculate δ directly from Eqs. (6)–(9). A simple expression for p_0 is derived for the autoresonance case, by neglecting u_2,

$$p_0=\frac{2r_e}{3}(\dot{\gamma}^2(1+L_0^2)+\gamma^4\{\dot{u}_1^2+[k_0(1-u_3)u_1]^2\}), \tag{53}$$

where we have used [see Eq. (36)]

$$\dot{\gamma}=\gamma^3(u_3\dot{u}_3+u_1\dot{u}_1),$$

$$\dot{u}_3=\frac{L_0}{\gamma^2}\dot{\gamma}.$$

Employing Eq. (36) one also gets

$$\dot{u}_1=-\frac{1}{8k_0\alpha_2\gamma^2}\left[A_1+\frac{2A_2}{\gamma}\right]$$

which on using $\Omega_0=-k_0L_0$ yields

$$p_0=\frac{2r_e}{3}\left\{\frac{(1+L_0^2)}{4\gamma}\left[A_1+\frac{A_2}{\gamma}\right]+\left[\frac{1}{8k_0\alpha_2}\left[A_1+\frac{2A_2}{\gamma}\right]\right]^2+\frac{\Omega_0^2}{(2k_0\alpha_2)^2}(A_1\gamma+A_2)\right\}. \tag{54}$$

Thus, we find that the first term in the right-hand side of Eq. (54) decreases as γ increases while the second and the third terms approach a constant value and increase linearly with γ, respectively. Therefore, for large enough γ ($\gamma\gg\gamma_0$),

$$p_0\approx\frac{4r_e}{3}\Omega_0^2L_0\gamma, \tag{55}$$

and from Eqs. (40) and (51),

$$\delta\approx 2\cdot 10^{-13}\frac{[\,|\Omega_0(\mathrm{cm}^{-1})|\,]^{5/2}\gamma^{3/2}}{[k_0(\mathrm{cm}^{-1})]^{3/2}\alpha_2}. \tag{56}$$

Therefore radiation losses put a limit on the maximum energy attainable in the ALA scheme

$$(mc^2)\gamma_{\max}\,(\mathrm{TeV})\sim 10\frac{\alpha_2}{[\lambda_0(1\ \mathrm{mm})]^{3/2}[B_z\,(100\ \mathrm{kG})]^{5/2}}. \tag{57}$$

We solved Eqs. (50) and (51) numerically with the equations of motion (6) through (11) and obtained general agreement between the results and the approximate Eq. (57). Thus, in conclusion, radiation losses seem to be negligible for a TeV ALA.

In the remaining part of this section we discuss the radial space charge effects on the performance of the ALA. Consider a homogeneous electron beam with density n and radius R_b propagating along a constant axial magnetic field, $\Omega_0=k_0\gamma_0(1-u_{30})$. As before we neglect the dispersion characteristics of the beam but nevertheless attempt to include small self-space-charge effects on the beam dynamics. Assume as a first approximation that the radial electrostatic field can be modeled according to

$$\mathbf{E}_r=-2\pi ne\mathbf{r}=\frac{2J\mathbf{r}}{cR_b^2}, \tag{58}$$

where J is the beam current, and $u_3\simeq 1$. Then, for $u_p=1$, the approximate equations of motion are

$$(\gamma u_1)^{\cdot}=a_0u_2+k_0\alpha_2(1-u_3)+a_rr_1, \tag{59}$$

$$(\gamma u_2)^{\cdot}=-a_0u_1+a_rr_2, \tag{60}$$

$$(\gamma u_3)^{\cdot}=k_0\alpha_2u_1, \tag{61}$$

$$\dot{\gamma}=\omega_0\alpha_2u_1+a_r(r_1u_1+r_2u_2), \tag{62}$$

where

$$a_r\equiv\frac{e\,|E_r|}{mc^2r}=\frac{0.12\,|J\,(\mathrm{kA})|}{[R_b\,(\mathrm{cm})]^2}\ \mathrm{cm}^{-2}. \tag{63}$$

Therefore if $a_rR_b\ll k_0\alpha_2$, or equivalently

$$J\,(\mathrm{kA})\ll 8k_0R_b, \tag{64}$$

then the acceleration gradients and the resonance condition do not change significantly as one moves from the axis to the edge of the beam. In general, for larger radii beams, higher currents are allowed by Eq. (64).

More accurate predictions on the influence of the space charge can be obtained by solving Eqs. (59)–(61) numerically. Results of such calculations for $B_z=100$ kG, CO_2 laser with $\alpha_2=1$, and electron beam with $R_b=1$ cm, $J=1$ kA, and $\gamma_0=50$ are shown in Fig. 5. This figure includes the variation of γ and the radius $r=(r_1^2+r_2^2)^{1/2}$ versus z for three different initial radii of an electron in the beam, namely 0,0.5,1 cm. In spite of the high current, as one can see in the figure, the autoresonance condition is approximately preserved. Nevertheless, we find a spread $\Delta\gamma$ in the final energies of electrons at different radii. In the above example $(\Delta\gamma/\gamma)<0.03$ after 100 cm of acceleration.

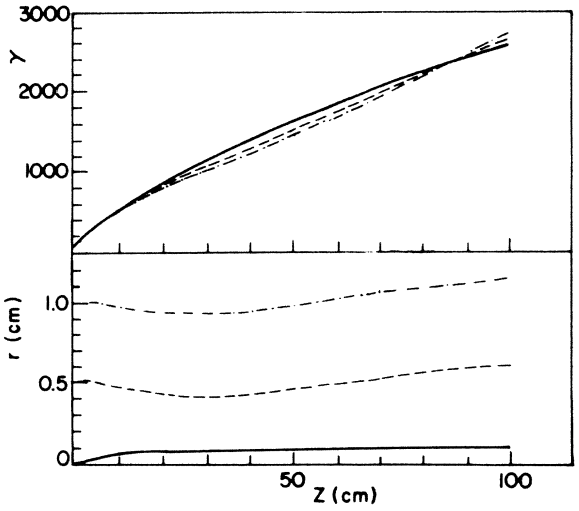

FIG. 5. Radial space-charge effects on acceleration. The dependence γ vs z is shown for three representative electrons with different initial radii: r_0. Scalloping of the beam is also demonstrated in the figure by showing the z dependence of the distance of the three electrons from the axis of symmetry (r). The parameters are $\lambda_0=10$ μm, $J=1$ kA, $R_b=1$ cm, $\alpha_2=1$, and $r_0=0$ (solid lines), $r_0=0.5$ cm (dashed lines), and $r_0=1$ cm (dot-dashed lines).

V. CONCLUSIONS

The ALA scheme, as described, is capable, in principle, of accelerating electron beams to the TeV energy range with low radiation losses. As a result of the homogeneity of the fields at the autoresonance condition for luminous radiation ($u_p=1$), acceleration of large-radii–high-current beams is feasible. Autoresonance acceleration of beams with low initial energy ($\gamma_0\sim 1$) is possible by using mm-wavelength radiation. This suggests a possibility of a multistage ALA with different γ_0 and corresponding k_0, at each stage. The autoresonance solution, as described in Eqs. (33)–(38) is not sensitive to the initial beam parameters when $\gamma \gg \gamma_0$. Furthermore, an electron beam with initially zero transverse momentum will be accelerated perpendicularly and "trapped" in phase with the laser radiation, if the resonance condition $\Omega=k_0/[(1+u_{30})\gamma_0]$ is satisfied initially. Therefore an output beam from a conventional linear accelerator with no transverse velocity can be injected and accelerated in the ALA.

The features of the ALA demonstrated above makes it attractive in comparison with the inverse FEL accelerator

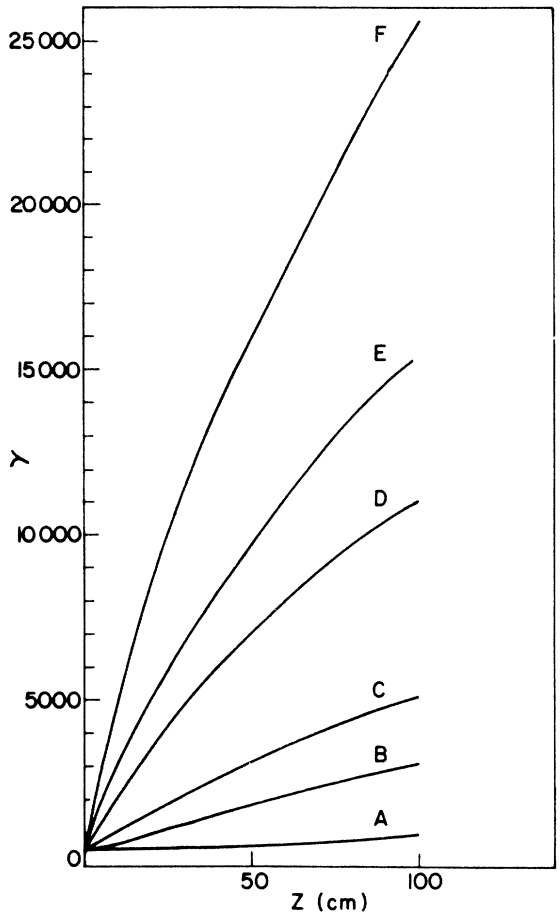

FIG. 6. The dependence of γ vs z on the strength of the electromagnetic wave in the ALA scheme for the luminous case with $\lambda_0=1$ μm, $\gamma_0=500$, $B_z=100$ kG, and A, $\alpha_2=0.1$; B, $\alpha_2=0.5$; C, $\alpha_2=1$; D, $\alpha_2=3$; E, $\alpha_2=5$; F, $\alpha_2=10$.

which suffers from phasing problems (only electrons in a certain phase with respect to the radiation can be accelerated in the IFEL scheme). In contrast to the PBWA where a saturation of the acceleration gradient occurs at a certain value of α_2 depending on k_0 and the density of the plasma,[12] the ALA scheme allows an increase in the acceleration rate by using large amplitude ultrarelativistic pulses (i.e., with $\alpha_2>1$). Figure 6 indicates the advantage of using ultrarelativistic pulses in the ALA scheme, where for $\lambda_0=1$ μm, $B_z=100$ kG, and $\alpha_2=10$, one can accelerate high-current electron beams from 0.25 to 12.85 GeV within the first meter of acceleration.

[1]*Proceedings of the Conference on Laser Acceleration of Particles,* AIP Conf. Proc. No. 91, edited by P. J. Channel (AIP, New York, 1982).

[2]T. Tajima and J. M. D. Dawson, Phys. Rev. Lett. **43**, 267 (1979).

[3]T. Katsouleas and J. M. Dawson, Phys. Rev. Lett. **51**, 392 (1983).

[4]C. Joshi *et al.*, Nature (London) **311**, 525 (1984).

[5]C. M. Tang, P. Sprangle, and R. Sudan, Appl. Phys. Lett. **45**, 375 (1984).

[6]C. Pellegrini, in *Proceedings of the Conference on Laser Acceleration of Particles,* AIP Conf. Proc. No. 91, edited by P. J. Channel (AIP, New York, 1982), pp. 138–153.

[7]C. S. Roberts and S. J. Buchsbaum, Phys. Rev. A **135**, 381 (1964).

[8]K. S. Golovanivsky, IEEE Trans. Plasma Sci. PS-11, **1**, 28

(1983).
[9]L. Friedland, Phys. Fluids **23**, 2376 (1980).
[10]A. Goldring and L. Friedland, Phys. Rev. A **32**, 2879 (1985).
[11]J. D. Jackson, *Classical Electrodynamics* (Wiley, New York, 1962), p. 470.
[12]T. Tajima, in *Proceedings of the 3rd Summer School on High Energy Particle Accelerators,* edited by M. Month (Brookhaven National Laboratory, Upton, New York, 1983), Vol. 1.